

## A SKIN FRICTION BALANCE APPLIED TO ROUGH WALL EXPERIMENTS

Vladislav Efros &amp; Per-Åge Krogstad

The Norwegian University of Science and Technology,  
N-7491 Trondheim, Norway

Corresponding author: vladislav.efros@ntnu.no

## ABSTRACT

This paper describes the design of a floating element friction balance which is based around a commercially available micro force balance. The balance has a perfectly linear calibration function and is very flexible as the measurement range may be varied by simply adjusting the length of one of the legs supporting the test surface.

The balance was successfully applied to rough wall flows in a channel and a diffuser. Both in the favourable pressure gradient flow of the channel and the adverse pressure gradient flow of the diffuser, extrapolation of the turbulent shear stress measured by two component LDA to the wall matched exactly the shear stress measured using the friction balance. Also, the wall shear stress obtained from the balance in the fully developed channel flow agreed with the stress that could be derived from the pressure gradient to within 3%.

## INTRODUCTION

The turbulent flow over rough surfaces has received considerable attention over the last two decades. One of the reasons is that the effect of the surface geometry on the outer flow appears to be an unresolved problem. According to Townsend's wall similarity hypothesis only a thin layer very close to the roughness elements should be directly influenced by the roughness geometry. Further away the flow is expected to be universal as sufficient number of eddy turnovers should ensure that the flow has forgotten the very nature that generated the turbulence. Hence from the log layer and out the flow is expected to be universal when properly scaled.

For boundary layers Krogstad and Antonia (e.g. Krogstad et al., 1992, and Krogstad and Antonia, 1999) have challenged this hypothesis and claimed that for certain roughness geometries both the mean velocity and turbulent stress profiles in the outer layer are significantly affected even when scaled with the appropriate similarity variables. The mean velocity wake was found to be stronger than over smooth surfaces and all stresses were increased all the way to the boundary layer edge. This observation has received support from some experimental investigators (e.g. Keirsbulck et al., 2002, Tachie et al., 2003) while others claim there is no outer layer effects (e.g. Flack et al., 2005, and Wu and Christensen, 2007). Quite recently Lee and Sung (2007) using DNS have given strong support to the outer layer effects previously observed in some experiments on roughness consisting of spanwise rods.

One possibility for the opposing observations may be that the effects depend on the actual surface geometry and type of flow considered as has been claimed by Krogstad et al. (2005). They investigated the flow in a 2D channel both experimentally and with DNS where the surface roughness consisted of spanwise rods and did not find the outer layer effects that had previously been reported for rod roughness in boundary layers.

The main scaling parameter for the mean flow and the turbulent stresses is the friction velocity. Experimentally this is

a quantity which is quite difficult to measure directly. Traditionally it has been determined for smooth wall experiments by fitting the data to the law of the wall

$$\frac{U}{u_\tau} = \frac{1}{\kappa} \ln \left( \frac{y u_\tau}{\nu} \right) + A \quad (1)$$

Here  $U$  is the mean velocity,  $y$  the distance from the wall and  $u_\tau$  the unknown friction velocity. Since the equation only contains one unknown the fit is reasonably accurate and straight forward if the log law constants,  $\kappa$  and  $A$ , are known precisely.

However, for rough walls the equation reads

$$\frac{U}{u_\tau} = \frac{1}{\kappa} \ln \left( \frac{[y + \epsilon] u_\tau}{\nu} \right) + A - \Delta U^+ \quad (2)$$

where  $\epsilon$  is the shift in origin from the measurement coordinate system to the effective wall location and  $\Delta U^+$  is the shift in the log law due to the roughness effect on the mean flow. Both are additional unknowns and makes the fitting process considerably more challenging. Therefore it is possible that some of the contradicting observations may in fact be due to the increased complexity in finding the scaling variable,  $u_\tau$ .

In order to reduce this uncertainty we have undertaken the process of trying to measure the wall friction directly using a friction balance. The operating principle of the balance is described in the next section. A direct local measurement is not possible but in slowly developing flows a locally averaged friction measurement may be performed by measuring the force on a limited surface area. If the flow can be assumed to be spanwise invariant the area can be extended in the spanwise direction and reduced in the streamwise direction so that the streamwise averaging distance may be kept quite small.

Although the friction force acting on a finite element of the surface is quite small, the measurement problem is considerably reduced on a rough surface due to the much higher forces caused by the additional pressure drag on the roughness elements compared to only viscous drag on a smooth surface. This may easily double or triple the wall friction force, making the surface stress measurements more reliable on rough than on smooth surfaces.

## DESCRIPTION OF THE BALANCE

The operating principle of the balance is shown in the Fig.(1). The device is of a single-pivot type and consists of two main parts:

- The sensing element, which consists of a replica of the test surface mounted on a thin plate (1). We have developed our balance for channel flow and two-dimensional boundary layer applications taking advantage of the spanwise homogeneity, so the sensing element is a rectangle with dimensions 50x350mm in the streamwise and spanwise directions, respectively. The test plate is mounted on a vertical frame (2) which rests on two knife edges. An adjustable horizontal bar (3) with two counter weights is

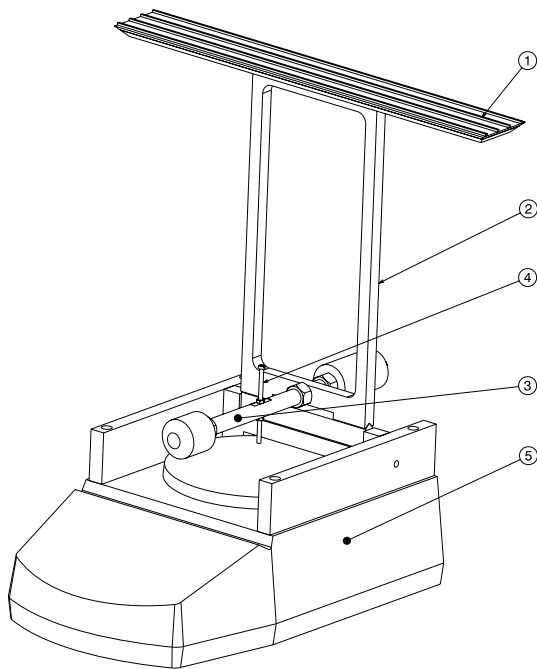


Figure 1: The skin friction balance.

connected to the lower part of the frame. The force is then transmitted to the sensing element through the adjustable vertical arm (4). By varying the ratio between arms (2) and (3) the "gain" of the system may be varied. The counter weights have been used to preload the sensing element of the balance to ensure that the balance always operates in its linear range.

- The balance (5) is a commercially available force sensing unit from Ohaus with a sensitivity of  $10^{-5}$ N. Normal loads on the test surface are typically of the order of 0.1N which are amplified through the mechanical "gain" (by a factor 5 in the present applications). Hence the measurement resolution was typically  $2 \cdot 10^{-5}$  of the applied load. For these forces the vertical motion of the sensing unit was less than  $100 \mu\text{m}$  as measured using a micrometer dial gauge.

In unloaded condition the test surface was centered in the slot cut in the floor of the wind-tunnel. The gap between the movable plate and the surrounding wall was nominally 0.6mm all around. The whole balance could be positioned very accurately by means of four screws controlling the vertical movement and two screws which could be used to shift the balance in the horizontal plane. (The adjustment screws are not shown in the figure.) In addition the sensing element could be accurately positioned in the streamwise direction by means of the vertical arm (4).

In order to reduce the effects of any flow through the gaps, the balance was mounted in a sealed box fitted under the test surface. Also to reduce the influence of pressure gradient forces acting on the sensing element substrate, the sensing element was milled to a sharp leading and trailing edge.

The balance was calibrated in situ in the wind tunnel. The main problem in calibrating the balance was to generate a well defined small force which is acting parallel to the test surface. This was solved by using a calibrating device constructed in a similar way as the arms of the balance, except that it was inverted. A balanced horizontal bar mounted on knife edges

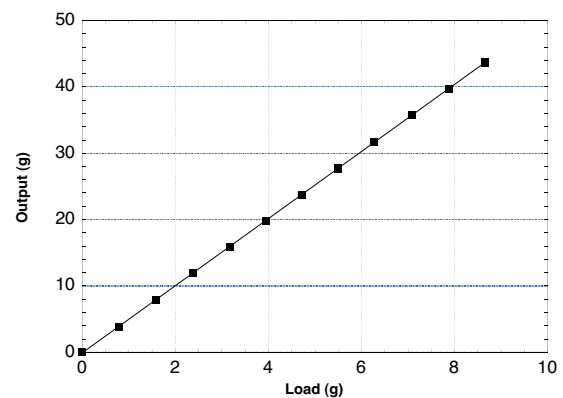


Figure 2: The calibration curve for the balance.

could be loaded with known masses on one end like an old-fashioned mechanical lab micro scale. A vertical lever extended down from the bar and was allowed to touch the test surface. In this way the calibration device was transferring the vertical force due to weights to a force in the horizontal direction.

The calibration curve obtained in this way is shown in Figure 2. The calibrated output is seen to be perfectly linear with very little scatter. The ratio between the two arms (2) and (3) in Figure 1 was adjusted to be close to 5:1 for the present applications and this may be seen to be reflected in the five times higher indicated output load from the balance than the applied calibration load. The linear calibration function fitted to the data was found to have a scatter typically less than 0.35% of the full load applied.

## RESULTS

The balance measures a combination of viscous- and pressure-drag acting on the test surface. On a rough surface the contribution from the pressure drag may be significantly larger than the viscous drag. The total drag was converted to an effective wall shear stress, i.e.

$$\tau_{wall} = F/A \quad (3)$$

where,  $F$ , is the force obtained from the balance.

The experiments were conducted in a closed return wind-tunnel. The test surfaces were the same as used by Krogstad et al. (2005). Both the roof and the floor were covered with square rods  $1.7 \times 1.7 \text{mm}^2$ . The pitch-to-height ratio  $\lambda/k$  was 8, which has been shown to produce k-type roughness. The upper wall of the wind-tunnel is adjustable, which allows the streamwise pressure gradient to be adjusted over a large range.

The measurement surface, extending 50mm in the streamwise direction, thus averages over less than 4 roughness periods.

Measurements of velocity field were performed using a Dantec two-components fiber-optic Laser Doppler Velocimeter (LDV). In order to do near-wall measurements the probe was tilted at a small angle. The flow was seeded with smoke particles provided by a Safex smoke generator. A total of 100 000 random velocity samples were obtained in coincidence mode for each location during the measurements. As in the previous study by Krogstad et al. (2005), all the measurements were taken above the crest of the roughness elements.

To determine  $u_\tau$  data from the balance was sampled on a separate PC for as long as the velocity measurement would take. Moving average calculations of the data from the balance

Case	h(cm)	$\beta$	$dP/dx$	$C_f$	Symbol
1	5	-1.027	< 0	0.0148	■
2	30	6.203	> 0	0.0048	●

Table 1: Parameters for experiment. The symbols shown are used in the plots.

showed that the stress measurements were always converged to within  $\pm 0.3\%$  of the final average.

In order to validate the accuracy of the balance we conducted two channel type experiments with quite different pressure gradients,  $dP/dx$ . The first experiment used the same setup as reported in Krogstad et al. (2005). This consists of a fully developed rough wall channel flow. The channel is 6m long, 1.4m wide with surface roughness on the roof and floor. The channel half height was  $h=0.05m$ . The flow for this case has been studied in detail before, both experimentally using hot wire anemometry and numerically using DNS. Being a fully developed channel flow the wall shear could also be determined accurately from the streamwise pressure gradient, i.e.

$$\tau_{wall} = h \cdot \frac{dP}{dx}, \quad (4)$$

which could be compared directly with the wall shear derived from the balance. The second advantage with a fully developed channel flow is that the shear stress distribution is uniquely defined by the equation

$$-\langle uv \rangle^+ = 1 + \beta \left( \frac{y^+}{h^+} \right) - \frac{dU^+}{dy^+} \quad (5)$$

where the superscript  $+$  indicates normalization with the shear velocity,  $u_\tau$ , and the viscous length scale,  $\nu/u_\tau$ .  $\beta$  is the non-dimensional pressure gradient

$$\beta = \frac{h}{\rho u_\tau^2} \cdot \frac{dP}{dx} \quad (6)$$

To measure the pressure gradient, the test section is fitted with pressure taps in the side wall on both sides, as well as along the the centerline of the floor at  $\Delta x = 20cm$  intervals. Theoretically  $\beta$  should be 1 for a fully developed channel flow, but by combining the pressure gradient from the pressure taps with the wall shear measured by the balance  $\beta$  was found to be -1.027. This indicates a combined error in the pressure and balance measurements of less than 3%.

In the other experiment the roof of the test section was raised to form a linear diffuser with the angle of the roof set at 3.3 degrees. In this way the flow is developing under an adverse pressure gradient. This should allow measurement errors on the balance performance caused by the pressure gradient to be detected since the sign has now been reversed. There is no equilibrium condition in this case, so the only verification that can be used is that the normalized shear stress extrapolates to 1 at the wall. For this flow  $\beta$  was about +6.2 at the measurement station, but varies with streamwise location.

A summary of the key data are given in Table 1. Going from the fully developed channel flow to the adverse pressure gradient diffuser the skin friction coefficient, here defined as  $C_f = 2\tau_{wall}/\rho U_c^2$  where  $U_c$  is the centre line velocity, decreased by a factor 3 and is here of the order of magnitude expected for zero pressure gradient boundary layers.

The mean velocity profiles for the two cases plotted in inner variables are shown in Figure 3. For reference the smooth wall log-law has been included. In both flows the centre line velocity was about the same, so the changes in the centre line  $U^+$  is roughly proportional to the changes in  $u_\tau$ . All cases show a

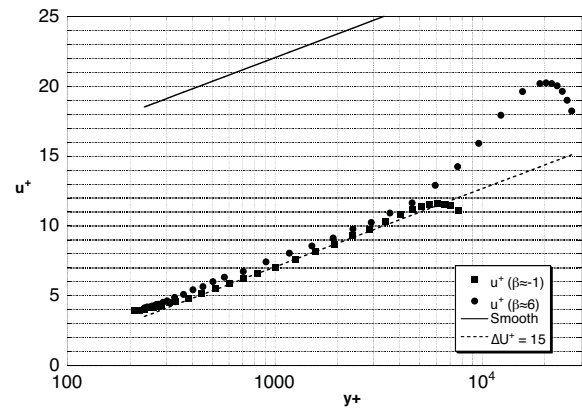


Figure 3: Mean velocity,  $U^+$ . Symbols as in Tab.1

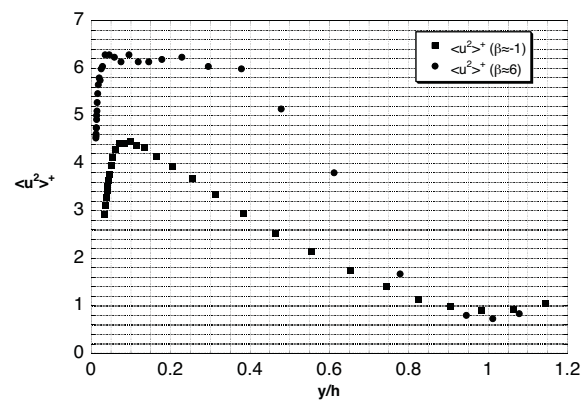


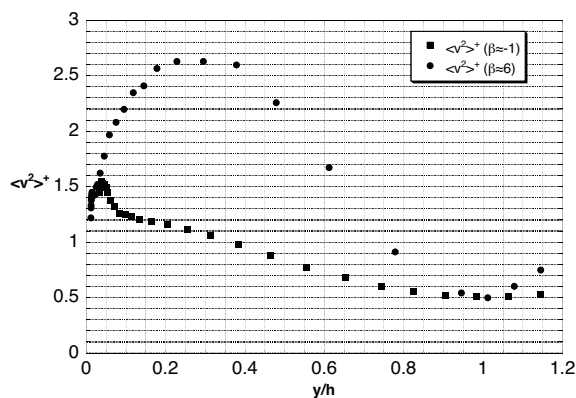
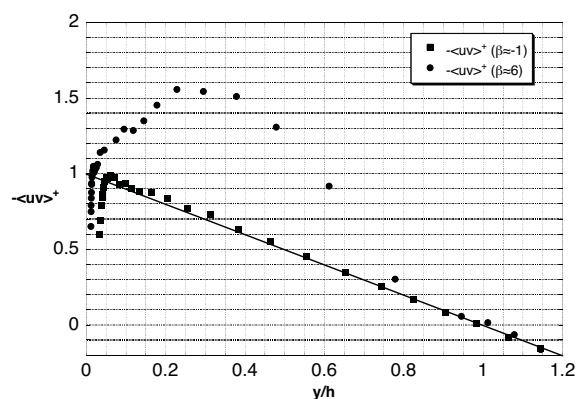
Figure 4: Normal stress,  $uu^+$ . Symbols as in Tab.1

linear log region with a shift in the log-law,  $\Delta U^+$ , of the order of 15. In the channel flow the shift was found to be  $\Delta U^+ \approx 15.0$  for  $k^+ = 210$  and in the adverse pressure gradient flow  $\Delta U^+ \approx 14.4$  at  $k^+ = 113$ . Hence it appears that the drag effect on the mean flow appears to be insensitive to the pressure gradient.

The normal stresses in outer coordinates are shown in Figures 4 and 5. The stresses at the center line are independent of the pressure gradient in the channel. However, it is apparent that both  $\langle u^2 \rangle^+$  and  $\langle v^2 \rangle^+$  are considerably increased throughout most of the layer. This is due to the increased turbulence production away from the surface in the case of an adverse pressure gradient. Figure 3 indicates that the mean velocity gradient,  $dU/dy$  is higher in the adverse pressure gradient flow than for the favourable pressure gradient channel flow case for most of the outer  $y/h$  region. Combined with a significant increase in the outer layer shear stress (Figures 6) this increases production in the transport equation for  $\langle u^2 \rangle^+$  which indirectly increases  $\langle v^2 \rangle^+$  through the pressure strain term.

The correlation coefficient,  $R_{uv} = -\langle u^2 \rangle^+ / \sqrt{\langle u^2 \rangle^+ \langle v^2 \rangle^+}$  is seen to be virtually identical for the two flows except very near the wall (Figures 7). This agrees with the findings of Skåre and Krogstad (1994) that the correlation coefficient is very little affected by pressure gradient effects.

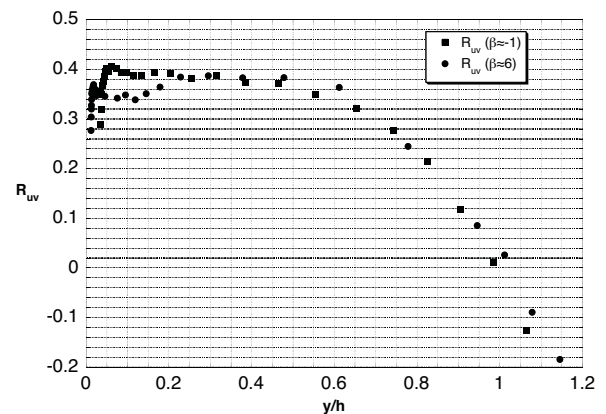
## DISCUSSION AND CONCLUSIONS

Figure 5: Normal stress,  $\langle v^2 \rangle^+$ . Symbols as in Tab.1Figure 6: Shear stress,  $\langle uv \rangle^+$ . Symbols as in Tab.1

The shear stress profiles measured over the same rough surface used in a fully developed channel flow and an adverse pressure gradient diffusor flow are shown in Figure 6. The measurements have been done with a two-component LDA system, but the data have been scaled with the friction velocity obtained from direct drag measurements on a small element of the surface. For the channel data we have added the theoretical straight line distribution for comparison. The agreement is seen to be excellent giving confidence to the direct drag measurements. For the adverse pressure gradient case the shear stress data is seen to grow linearly near the wall as expected and this data set also extrapolates back to 1 at the wall when scaled with the balance measurements.

We therefore suggest that the balance designed and described in this paper can be used to give reliable results for the wall shear stress on rough walls. So far the balance has only been used for rough wall flows since the wall shear is considerably higher in this case than for a smooth wall. However, the data obtained in the adverse pressure gradient flow gave a value for the friction coefficient which is not too different from what is to be expected for smooth wall zero pressure gradient flows, so we are quite optimistic that the balance may also prove useful for smooth wall experiments.

Direct floating balance friction measurements are not a new technique. What makes the present design unique is that instead of trying to design all components for a complete balance from scratch, we have chosen to use an "off the shelf" micro

Figure 7: Correlation coefficient,  $R_{uv}$ . Symbols as in Tab.1

force measurement unit with proven accuracy and stability for the sensing part and concentrated on designing the elements needed to pick up the force and transmit it to the force sensor. By using this strategy we have managed to produce a force balance with very high resolution and excellent linearity. The system also includes a mechanical "variable gain" geometry which makes it possible to tune the characteristics of the balance to the application.

## REFERENCES

- Krogstad, P.-Å., Antonia, R.A. and Browne, L.W.B., 1992, "Comparison between rough- and smooth-wall turbulent boundary layers", *J. Fluid Mech.* **245** pp. 599–617
- Krogstad, P.-Å. and Antonia, R.A., 1999, "Surface roughness effects in turbulent boundary layers", *Exp. Fluids* **27** pp. 450–460
- Keirsbulck, L., Labraga, L., Mazouz, A. and Tournier, C., 2002, "Surface roughness effects on turbulent boundary layer structure", *J. Fluids Eng.* **124** pp. 127–135
- Tachie, M.F., Bergstrom, D.J. and Balachandar, R., 2003, "Roughness effects in low- $Re_\theta$  open-channel turbulent boundary layers", *Exp. Fluids* **35** pp. 338
- Flack, K.A., Schulz, M.P. and Shapiro, T.A., 2005, "Experimental support for Townsends Reynolds number similarity", *Phys. Fluids* **035102**
- Wu, Y. and Christensen, K.T., 2007, "Outer-layer similarity in the presence of a practical rough-wall topography", *Phys. Fluids* **19** 085108
- Lee, S.-H. and Sung, H.J., 2007, "Direct numerical simulation of the turbulent boundary layer with rod-roughened wall", *J. Fluids Eng.* **584** pp. 125–146
- Krogstad, P.-Å., Andersson, H. I., Bakken, O.M. and Ashrafian, A., 2005, "An experimental and numerical study of channel flow with rough walls", *J. Fluid Mech.* **530** pp. 327–352
- Acharya, A. and Escudier, M. P., "Measurements of the Wall Shear Stress in Boundary Layer Flows", *Turbulent Shear Flows* **4** pp. 277–286
- Karlsson, Rolf, I., "Studies of skin friction in turbulent boundary layers on smooth and rough walls"
- Flack, K.A., Schulz, M.P. and Connelly, J.S., 2007, "Examination of a critical roughness height for outlet layer similarity", *Phys. Fluids* **19** 095104
- Skåre, P.E. and Krogstad, P.-Å., 1994, "A turbulent equilibrium boundary layer near separation", *J. Fluid Mech.* **272** pp. 319–348